Effect of Contact Statistics on Electrical Contact Resistance

YongHoon Jang†

전기접촉저항에 관한 접촉통계치의 영향

장용훈

Key Words: Electrical contact resistance(전기접촉저항), Microcontact distribution(미소접촉분포), Multiscale analysis(멀티스케일해석), Fractal surface(프랙탈 표면)

Abstract

The flow of electrical current through a microscopic actual contact spot between two conductors is influenced by the flow through adjacent contact spots. A smoothed version of this interaction effect is developed and used to predict the contact resistance when the statistical size and spatial distribution of contact spots is known. To illustrate the use of the method, an idealized fractal rough surface is defined using the random midpoint displacement algorithm and the size distribution of contact spots is assumed to be given by the intersection of this surface with a constant height plane. With these assumptions, it is shown that including finer scale detail in the fractal surface, equivalent to reducing the sampling length in the measurement of the surface, causes the predicted resistance to approach the perfect contact limit.

1. Introduction

When two large conductors make perfect electrical contact over a small circular area of radius *a,* there will be a *constriction resistance* to electrical flow between them of $\rho/2a$, where ρ is the electrical resistivity. This equation is widely used in the design and study of electrical contacts. However, if the contacting bodies have rough surfaces, contact will rarely be restricted to a single area. Instead, there will be contact at a multitude of microscopic `actual' contacts clustered within a macroscopic `nominal' or `apparent' contact area. Greenwood[1] has analyzed such clusters, treating a number of distributions of size and spacings, and has confirmed an earlier suggestion by Holm[2] that the combined effect of the local constriction and the clustering is to generate a resistance

$$R = \rho\left(\frac{1}{2Na} + \frac{1}{2\alpha}\right) \qquad (1)$$

where N is the number of circular contact spots and α is the radius of the cluster.

Many authors have attempted to generalize Greenwood's results to define the electrical and thermal conductance in the presence of clusters of microcontacts. Contact resistance has been computed numerically by Nakamura[3] for a system of two cubic electrodes contacting through a set of square contact spots, whilst Boyer[4] has extended the Greenwood formula to include the presence of interfacial films by considering the rectangular juxtaposition of square spots of equal size and square ring-shaped spots.

Eq. (1) provides a good approximation to the electrical contact resistance for a deterministic distribution of contact spots of known size and location, but information about the distribution of asperities is most likely to be statistical in nature, since surface roughness is essentially a random process. Furthermore, surface roughness descriptions are typically multiscale in nature and on a sufficiently fine scale, the number of discrete contact spots is likely to be too large to permit an efficient deterministic calculation. In the present paper, we shall develop a statistical version of Greenwood's equation, in which the summation is replaced by an integral over the nominal contact area with a kernel that depends on the statistical properties of the distribution. We shall then test the predictions of the theory by comparison with a discrete deterministic realization developed using the random mid-point displacement algorithm. In particular,

† 연세대학교 공과대학 기계공학부
E-mail : jyh@yonsei.ac.kr
TEL : (02)2123-5812 FAX : (02)312-2159

we shall investigate the effect on the predicted contact resistance of the sampling length on the model surface, using recent results due to Jang[5] for relations between two and three-dimensional properties of random surfaces.

2. Statistical Implementation of Greenwood's equation

Greenwood's result is based on the approximation of the potential field due to current flow through a microscopic contact spot by that due to a point current source in all locations other than the immediate vicinity of the contact spot. Thus, the potential ϕ_j at the j-th contact spot in a set of N randomly disposed contact spots as shown in Fig. 1 is

$$\phi_j = \frac{\rho I_j}{4a_j} + \frac{\rho}{2\pi}\sum_{i\neq j}\frac{I_i}{s_{ij}} \tag{2}$$

where I_i is the current through the i-th contact spot, a_i is its radius, s_{ij} is the distance from between the centers of the i-th and j-th contact spots and the summation is performed over all the N contact spots *except* $i=j$.

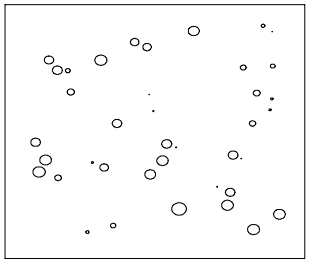

Fig. 1 Configuration of contact

2.1 The base potential

We will define the *base potential* $\overline{\phi}_j$ through the relation (2)

$$\overline{\phi}_j \equiv \phi_j - \frac{\rho I_j}{4a_j} = \frac{\rho}{2\pi}\sum_{i\neq j}\frac{I_i}{s_{ij}}. \tag{3}$$

With this notation, we have

$$I_j = \frac{4a_j}{\rho}(\phi_j - \overline{\phi}_j) \tag{4}$$

and using this result to substitute for I_i in Eq. (3), we obtain

$$\overline{\phi}_j = \frac{2}{\pi}\sum_{i\neq j}\frac{a_i(\phi_i - \overline{\phi}_i)}{s_{ij}}. \tag{5}$$

2.2 Integral form of the equation

Suppose that in some nominal area *A*, there exists a single circular contact spot and that the probability of its radius being between *a* and $a+\delta a$ and of its center being located in the rectangle defined by the lines $x, x+\delta x, y, y+\delta y$ is $h(x, y, a)\delta x\delta y\delta a$ where *h(x,y,a)* is a probability distribution function which satisfies the equation

$$\iint_A [\int_0^\infty h(x, y, a)\, da]\, dxdy = 1. \tag{6}$$

A similar definition can be used for the case where there are *n* contact spots per unit nominal area, in which case the probability of a contact spot of radius $a+\delta a$ having its center within the infinitesimal rectangle will be $nAh(x, y, a)\, dadxdy$. This definition implicitly assumes that the distribution is uncorrelated - i.e., that the probability of a contact spot at (x,y) is unaffected by the actual occurrence of a contact spot at a nearby point. The consequences of this assumption will be discussed in Section 7.

The base potential at the point *x,y* due to the distribution *h(x,y,a)* can now be written

$$\overline{\phi}(x,y) = \iint_A\int_0^\infty \frac{2nAh(\xi,\eta,a)(\phi(\xi,\eta)-\overline{\phi}(\xi,\eta)a\,da\,d\xi\,d\eta}{\pi\sqrt{(x-\xi)^2+(y-\eta)^2}} \tag{7}$$

where the domain of integration is the nominal contact area and the range of contact spot radii.

If the integral with respect to *a* can be performed, defining the new function

$$\overline{h}(\xi,\eta) \equiv \int_0^\infty nAh(\xi,\eta,a)\,a\,da \tag{8}$$

then

$$\overline{\phi}(x,y) = \iint_A \frac{2\overline{h}(\xi,\eta)(\phi(\xi,\eta)-\overline{\phi}(\xi,\eta)d\xi d\eta}{\pi\sqrt{(x-\xi)^2+(y-\eta)^2}} \tag{9}$$

2.3 The Boundary Value Problem

If two half spaces make electrical contact at a number of areas on their common plane surface, the potential problems in the two bodies will be geometrically similar and the actual contact areas will form an equipotential surface. In particular, the potential difference between this surface and the extremity of body *i (i=1,2)* will be

$$\phi = \frac{U\rho_i}{\rho_1+\rho_2}, \tag{10}$$

where ρ_i denotes the resistivity of the material of body *i* and *U* is the potential difference between the extremities of the two bodies. In more general problems, ϕ may not be constant. For example, if one of the bodies conducts a current in a direction tangential to the common interface, ϕ will be a linear function of ξ, η..

Thus, $\phi(\xi,\eta)$ is a known function, as is $h(\xi,\eta,a)$, and hence we can determine the function

$$f(x,y) \equiv \iint_A \frac{2\overline{h}(\xi,\eta)\phi(\xi,\eta)\,d\xi\,d\eta}{\pi\sqrt{(x-\xi)^2+(y-\eta)^2}} \tag{11}$$

It follows that the base potential $\overline{\phi}$ is the solution of

$$\iint_A \frac{2\bar{h}(\xi,\eta)\bar{\phi}(\xi,\eta)\,d\xi\,d\eta}{\pi\sqrt{(x-\xi)^2+(y-\eta)^2}} + \bar{\phi}(x,y) = f(x,y) \tag{12}$$

which is a singular integral equation of the second kind, for which various solution methods are available.

Once $\bar{\phi}(x,y)$ has been determined from this equation, the current through each individual contact spot is defined in the discrete formulation of Eq. (4) so that the current through all contact spots can be summed as

$$I \equiv \sum_{j=1}^{N} I_j = \sum_{j=1}^{N} \frac{4a_j}{\rho}(\phi_j - \bar{\phi}_j). \tag{13}$$

The integral form of this equation can be written as

$$I = \frac{4}{\rho}\iint_A \int_0^\infty nAh(\xi,\eta,a)(\phi(\xi,\eta)-\bar{\phi}(\xi,\eta))\,a\,da\,d\xi\,d\eta$$

$$= \frac{4}{\rho}\iint_A \bar{h}(\xi,\eta)(\phi(\xi,\eta)-\bar{\phi}(\xi,\eta))\,d\xi\,d\eta \tag{14}$$

We can also define the local mean current density as

$$i(x,y) = \frac{4}{\rho}\bar{h}(x,y)(\phi(x,y)-\bar{\phi}(x,y)) \tag{16}$$

Notice that *i(x,y)* is averaged over the local discontinuities associated with the actual contact areas, but it will vary over the nominal contact area. Statistically, it can also be regarded as the expected value of current density at the point *(x,y)*.

3. Interpretation of the Function $\bar{h}(\xi,\eta)$

Suppose that the spatial distribution of contact spots and the size distribution are uncorrelated, so that $h(\xi,\eta,a)$ can be written in the normalized separated variable form

$$h(\xi,\eta,a) = h_1(\xi,\eta)h_2(a) \tag{17}$$

where

$$\int\int_A h_1(\xi,\eta)\,d\xi\,d\eta = 1;\ \int_0^\infty h_2(a)\,da = 1 \tag{18}$$

We then have

$$\bar{h}(\xi,\eta) = nAh_1(\xi,\eta)\int_0^\infty h_2(a)a\,da = nAh_1(\xi,\eta)\bar{a} \tag{19}$$

from Eq. (12), where $\bar{a}$ is the mean value of *a*. If the distribution function $h_1(\xi,\eta)$ is uniform in *A*, we have

$$h_1(\xi,\eta) = \frac{1}{A} \tag{20}$$

from (18) and hence

$$\bar{h}(\xi,\eta) = n\bar{a}\ . \tag{21}$$

More generally, the function $\bar{h}(\xi,\eta)$ is equal to the product of the number of contact spots per unit area and the mean radius, both of which may be functions of position.

4. Microcontact spot distribution

Eqs. (10, 12, 15) permit us to determine the electrical contact resistance

$$Re = \frac{U}{I} \tag{22}$$

for any rough surface contact problem, provided we can determine the corresponding statistical distribution functions $h_1(\xi,\eta)$ and $h_2(a)$. Various methods exist for this purpose.

For example, we might use an asperity model theory suchas those due to Greenwood and Williamson[6] for flat surfaces orGreenwood and Tripp[7] for non-conforming surfaces.

In the present paper, we shall illustrate the method by making the assumption that the distribution of contact spots is defined by the set of `islands' generated by cutting through the rough surface at constant height. This assumption was used by Majumdar and Bhushan[8] in their fractal theory of contact and is related to the concept of `bearing area' which is arguably appropriate when the contact deformations are predominantly plastic.

For this purpose, we generated a randomly rough surface using the r*andom midpoint displacement algorithm*(RMD) (Voss[9]). Suppose the values of the process are defined at the nodal points of a square grid. The grid is now sub-divided by introducing new nodal points at the mid points. The value of the process at each mid-point is determined as the sum of the average of the two adjacent end points and a zero mean random process with a Gaussian distribution. This procedure of subdivision is applied recursively and the standard deviation of the random process at each scale is chosen so as to ensure that the algorithm generates a self-affine fractal surface.

Starting with a square of dimension LxL, m applications of the algorithm will generate a square grid of $(2^m+1)\times(2^m+1)$, corresponding to a fractal surface measured with a sampling length of $L/2^m$.

Figure 2(a) shows a typical rough surface generated by this algorithm in the unit square and Fig. 2(b) shows the corresponding bearing area ratio *B(z)*. The bearing area ratio is defined as the proportion of the surface above the height *z*. The z-axis in these figures is normalized with respect to the standard deviation σ (i.e. the RMS roughness) of the resulting surface.

Figure 2(c) shows the contact spots defined by cutting through the surface at the level where the bearing area ratio is 5% (i.e. B(z)=0.05), with a grid size (sampling length) of $1/2^7$. A total of 27 contact spots are identified, but they are clearly not circular, as required by the analysis of section II. A distribution function for `equivalent' contact radii might be obtained by defining a set of circles whose areas are equal to that of the islands in Fig.

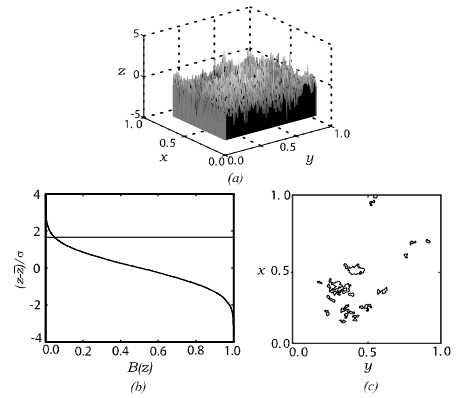

Fig. 2 Rough surface generated by the RMD algorithm. (a)three-dimensional view; (b) the corresponding bearing area ratio B(z); (c) the set of islands generated by cutting through the surface at B(z)=0.05.

2(c). However, we note that in most cases, the complete topographical description implied in Fig. 2(a) is not available. Instead, we typically have profilometer output, which is equivalent to a sampling of the surface along one or more lines. This permits the bearing area ratio (Fig. 2(b)) to be determined, but information about the distribution of islands $h_2(a)$ must be deduced from the corresponding distribution of line segments *f(l)* above a given height in the profile. Jang[5] has shown that a distribution $h_2(a)$ of circular contact spots will lead to a distribution *f(l)* of line segments above the specified height, where

$$h_2(a) = -\frac{2\bar{a}}{\pi}\frac{d}{da}\int_a^\infty \frac{f(l)}{\sqrt{l^2-a^2}}dl. \qquad (23)$$

and the mean radius of the circles is

$$\bar{a} = \pi/2\int_0^\infty \frac{f(l)}{l}\,dl\ . \qquad (24)$$

The number of contact spots \$n\$ per unit area is

$$n = \frac{2n_c}{\bar{a}}\ , \qquad (25)$$

where n_c is the number of the line segments per unit length[5].

To utilize the above equations, we first sample the model surface along a set of lines to measure the number of line segments per unit length n_c above a given height z and the length distribution of these line segments *f(l)*. Eq. (24) then allows us to evaluate the mean radius $\bar{a}$ of the contact spots in the corresponding three-dimensional section and Eq. (25) determines the number of contact spots per unit area, n. Finally, Eq. (23) determines the probability density of the distribution for the contact radius.

This method gives good results for the distribution of contact spot sizes as long as the bearing area ratio is less than 10%. For larger values of bearing area ratio, more complex contact spot geometries are obtained[5], some involving multiply connected areas - i.e. one or more regions of separation completely surrounded by contact. However, these conditions occur only under extremely high loads and are not of much practical interest.

5. Results

As an example problem, we consider the contact between two half spaces over a square nominal contact area of size 1 mm x 1mm at various values of the bearing area ratio B(z). The resistivity of both half spaces was taken to be $\rho_1 = \rho_2 = 25\times10^{-9}\,\Omega m$.

Figure 3 shows the variation of (a) the function $\bar{h} = n\bar{a}$ from Eq. (21) and (b) the electrical resistance *Re* with the bearing area ratio *B(z)*. As we would expect, the contact resistance decreases with increasing bearing area ratio. For comparison, Nakamura[3] showed that the electrical resistance for conduction through a single square contact spot of side L is

$$R_e^{SN} = \frac{0.868\rho}{L}\ . \qquad (26)$$

Thus, if there were perfect electrical contact over the entire nominal contact area, the resistance would be 21.7 $\mu\Omega$.

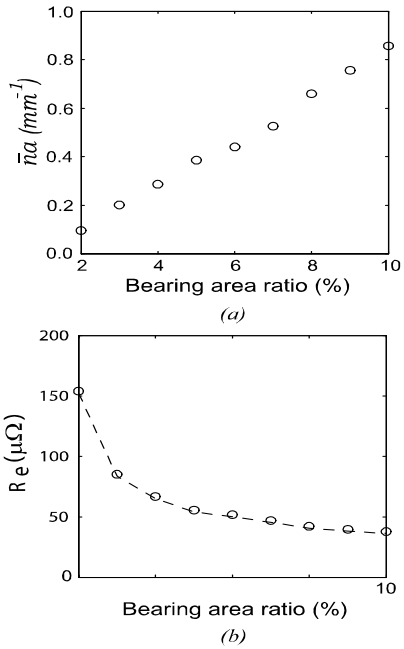

Fig. 3 Variation of (a) the function $\bar{h} = n\bar{a}$ from Eq. (21) and (b) the electrical contact resistance Re with bearing area ratio B(z). The dashed line in (b) was obtained from Eq. (27).

5.1 Comparison with Greenwood's equation

Eq. (1) applies specifically to the case of a circular

nominal contact area of radius α, containing a distribution of N contact areas, each of radius *a*. However, it is readily generalized to the present case by (i) replacing the cluster resistance term $\rho/2\alpha$ by R_e^{SN} of Eq. (26) and (ii) replacing the product *Na* by $L^2\bar{n}a$, giving

$$R_G = \frac{\rho}{L}\left(\frac{1}{2L\bar{n}a} + 0.868\right) . \qquad (27)$$

This simple expression is shown by the dashed line in Figure 3(b) and it clearly gives a very good approximation to the present numerical predictions. In fact, Eq. (27) is always slightly lower than the corresponding numerical calculation, the percentage difference being shown in Figure 4 as a function of $\bar{n}a$. The reason for this difference is that the numerical treatment allows for the effect of the microscopic resistance in modifying the mean current density in the `cluster-scale' problem, whereas Eq. (27) assumes that the cluster resistance is always that which would be obtained in the perfect contact problem. This is most significant when the microscopic resistance is large, in which case the mean current density will be approximately uniform in the nominal contact area, rather than having the square-root singular behaviour implied by Nakamura's solution[3] and Eq. (26). However, in this limit, the resistance is dominated by the microscopic resistance term and hence Eq. (27) still gives a good approximation to the numerical results. The maximum percentage difference therefore occurs at intermediate values of $L\bar{n}a$, being 3.86% at $L\bar{n}a$=1.35.

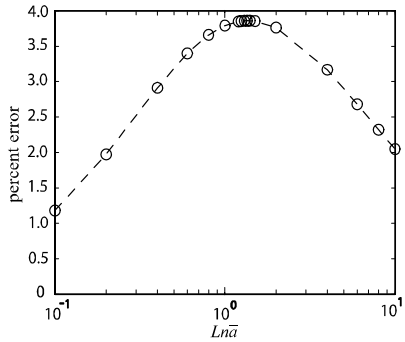

Fig. 4 Percentage difference between the predictions of the Greenwood equation (27) and the solution of section III as a function of $L\bar{n}a$.

5.2 Effect of sampling length

Experimental measurements with the stylus profilometer show that when using a large sampling interval, the surface exhibits only a few asperities with a large radius of curvature, whereas with a smaller sampling interval, larger numbers of asperities of smaller radius are revealed. Classical asperity-based models of contact appear to give reasonable predictions of electrical and thermal resistance, but it is not clear what sampling interval should be used in defining the resulting asperities. Ideally, we would hope that the predictions obtained using progressively refined surface descriptions would tend to a limit at small sampling length, thus providing some justification for truncating the description at a finite length scale.

This effect can be simulated in the present example by increasing the grid refinement of the RMD model. Figure 5(a) shows the function $\bar{h} = \bar{n}a$ from Eq. (21) as a function of grid refinement m for a bearing area ratio of 5%. This corresponds to the sampling of the rough surface at an interval of $1/2^m$ mm. The results show a considerable increase in $\bar{h}$ with increasing m and this translates to a comparable reduction of contact resistance *Re*, as shown in Fig. 5(b). The dashed line in Figure 5(b) corresponds to the Greenwood equation (27). These numerical calculations were extended to larger values of $\bar{n}a$ and confirm that the resistance tends to the perfect contact limit of Eq. (26) as $\bar{n}a \rightarrow \infty$.

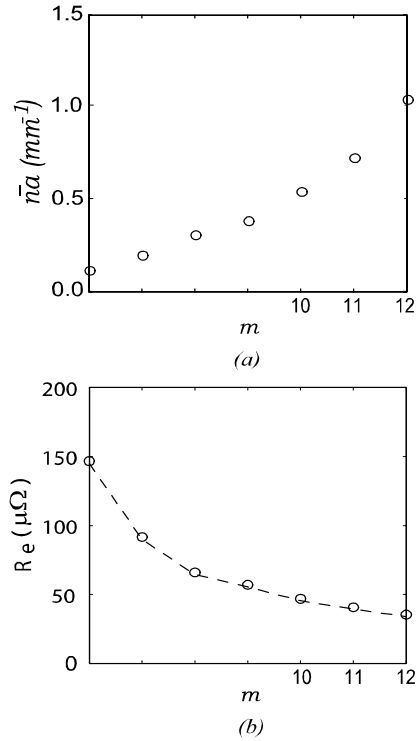

Fig. 5 Variation of (a) the function $\bar{h} = \bar{n}a$ from Eq. (21) and (b) the electrical contact resistance Re with sampling length $1/2^m$ for a bearing area ratio of 5%. The dashed line in (b) was obtained from Eq. (27).

6. Discussion

The multiscale model predicts a lower electrical contact resistance when a finer scale is used, since the finer scale reveals larger numbers of additional microscopic contact spots. In particular, the mean radius $\bar{a}$ decreases, but there is a larger increase in the number of contact spots per unit area *n*, leading to a net increase in $\bar{h}$. Similar behaviour has been reported in other recent studies of the contact of quasi-fractal surfaces.[10,11]

The `bearing area' hypothesis used in the example in section V predicts a distribution that contains a some relatively large contact spots along with increasingly large numbers of smaller spots as the sampling length is reduced. Similar characteristics are implied in the fractal contact model of Majumdar and Bhushan[8]. This theory is most appropriate when the microscopic problem is dominated by plastic deformation, since in this case each local asperity contact is analogous to a hardness indentation. By contrast, the elastic contact theories of Borri-Brunetto et. al.[10] and Ciaverella et. al[11] predict that the size of all contact spots decreases with decreasing sampling length, so that in the theoretical fractal limit we have an infinite number of contact spots of zero size.

Elastic fractal contact theories also show that the product $\bar{h} = n\bar{a}$ would be unbounded in the limit $m \to \infty$, whilst the total area of actual contact

$$A_c = \sum_{i=1}^{N} \pi a_i^2 \tag{28}$$

tends paradoxically to zero[14,15]. If we define a new function

$$\psi(\xi,\eta) \equiv \phi(\xi,\eta) - \bar{\phi}(\xi,\eta), \tag{29}$$

and use this expression and (19) to substitute to (9), we obtain

$$\int\int_A \frac{2\bar{h}(\xi,\eta)\psi(\xi,\eta)d\xi d\eta}{\pi\sqrt{(x-\xi)^2+(y-\eta)^2}} + \psi(x,y) = \phi(x,y) \tag{30}$$

Now if $\bar{h}(\xi,\eta)$ increases without limit, the left hand side of this equation becomes increasingly dominated by the first term and ψ will become small compared with ϕ. In the fractal limit, we would obtain $\psi = 0$ and hence $\phi = \bar{\phi}$. In other words, the base potential would become equal to the potential at the contact interface and Eqs. (16, 12) would give

$$\frac{\rho}{2\pi}\int\int_A \frac{i(\xi,\eta)d\xi d\eta}{\sqrt{(x-\xi)^2+(y-\eta)^2}} = \phi(x,y), \tag{31}$$

which is the equation defining perfect electrical contact throughout the nominal contact area A. Thus, any contact theory that predicts a distribution function $\bar{h} = n\bar{a}$ which increases without limit with decreasing sampling length will imply an electrical resistance equal to that based on the simple assumption of perfect electrical contact in the nominal contact area.

7. Conclusions

We have presented a model for the electrical contact of rough surfaces, extending Greenwood's equation for conduction through a cluster of circular contacts to a system in which the probability of a contact spot at a given location is defined in statistical terms. The model was illustrated using a mathematically generated surface with fractal characteristics and the bearing area hypothesis, properties of the surface being determined using a relation between three-dimensional properties and profile properties due to Jang[9]. We show that in the fractal limit the theory would predict effectively perfect electrical contact throughout the nominal contact area, suggesting that the correlation between the location of adjacent contact spots needs be taken into account.

Acknowledgement

This work was supported by grant No R08-2003-000-10162-0 from the Basic Research Program of the Korea Science & Engineering Foundation.

Reference

(1) J.A. Greenwood, 1966, "Constriction resistance and the real area of contact", *British Journal of Appied Physics,* Vol. 17, pp.1621-1632.
(2) R. Holm, 1967, Electrical Contacts, Theory and Applications, Springer-Verlag, Berlin..
(3) M. Nakamura, 1994, "Computer simulation for the constriction resistance depending on the form of conducting spots", *IEEE Trans. Comp., Packag., Manuf. Technol. A,* Vol. 18, pp.382-383.
(4) L. Boyer, 2001, "Contact resistance calculations: Generalizations of Greenwood's formula including interface films", *IEEE Trans. Comp., Hybrids, and Manufact. Technol.* Vol. 24, pp.50-58.
(5) Y.H. Jang, 2003, "Distribution of three dimensional Islands from two dimensional Line Segment Length Distribution", *Wear*, in submission.
(6) J.A. Greenwood and J.B.P. Williamson, 1966, "Contact of nominally flat surfaces", *Proc. R. Soc. London, Ser A* , Vol. 295, pp.300-319.
(7) J.A. Greenwood and J.H. Tripp, 1967, "The elastic contact of rough spheres", *J. Appl. Mech.* Vol. 34, pp.153.
(8) A. Majumdar and B. Bhushanm, 1991, "Fractal model of elastic-plastic contact between rough surfaces," *J. Tribol.,* Vol.113, pp.1-13.
(9) R.F. Voss, Fundamental Algorithms for Computer Graphics, edited by R.A. Earnshaw, NATO ASI Series F17 (Springer-Verlag, Berlin, 1985), pp.805--835.
(10) M. Borri-Brunetto, A. Carpinteri, B. Chiaia, *Probamat-21st Century: Probabilities and Materials*, edited by G. Frantziskonis, (Kluwer Academic Publishers, Dordrecht, 1998), pp.45--64.
(11) M. Ciaverella, G. Demelio, J.R. Barber, and Y.H. Jang, 2000, "Linear elastic contact of the Weierstrass profile," *Proc. R. Soc. London, Ser. A* Vol. 456, pp.387.